Pulsating Magnetic Reconnection Driven by Three-Dimensional Flux-Rope Interactions

W. Gekelman,[1] T. De Haas,[1] W. Daughton,[2] B. Van Compernolle,[1] T. Intrator,[2] and S. Vincena[1]
[1]Department of Physics, University of California, Los Angeles, Los Angeles, California 90095, USA
[2]Los Alamos National Laboratory, Los Alamos, New Mexico 87545, USA
(Received 18 December 2015; published 9 June 2016)

The dynamics of magnetic reconnection is investigated in a laboratory experiment consisting of two magnetic flux ropes, with currents slightly above the threshold for the kink instability. The evolution features periodic bursts of magnetic reconnection. To diagnose this complex evolution, volumetric three-dimensional data were acquired for both the magnetic and electric fields, allowing key field-line mapping quantities to be directly evaluated for the first time with experimental data. The ropes interact by rotating about each other and periodically bouncing at the kink frequency. During each reconnection event, the formation of a quasiseparatrix layer (QSL) is observed in the magnetic field between the flux ropes. Furthermore, a clear correlation is demonstrated between the quasiseparatrix layer and enhanced values of the quasipotential computed by integrating the parallel electric field along magnetic field lines. These results provide clear evidence that field lines passing through the quasiseparatrix layer are undergoing reconnection and give a direct measure of the nonlinear reconnection rate. The measurements suggest that the parallel electric field within the QSL is supported predominantly by electron pressure; however, resistivity may play a role.

DOI: 10.1103/PhysRevLett.116.235101

Introduction.—Flux ropes are magnetic structures with helical magnetic fields (and currents) and are known to occur throughout space and astrophysical plasmas [1]. Flux ropes routinely occur within Earth's magnetopause boundary layer and within the magnetotail. The surface of the Sun is littered with arched flux ropes. Some are stable and others can erupt resulting in coronal mass ejections (CMEs). Large CMEs have caused power outages and can populate Earth's radiation belts with high-energy ions and electrons that may damage or destroy satellites. When two or more flux ropes are close to one another, they will interact. The $\vec{J} \times \vec{B}$ force will cause ropes to twist about one another (and themselves). The ropes can merge as they attempt to achieve a force-free state. On the other hand, sheets of current can spontaneously form multiple flux ropes through the tearing instability [2]. The magnetic fields and associated current systems of flux ropes are quite complicated, and a complete study has to account for where they originate and how they close. Finally, flux ropes can be kink unstable. If adjacent ropes are unstable, they can collide when they kink, leading to sheared magnetic fields in the interaction regions, which are susceptible to magnetic reconnection. In the present study, this scenario is observed in a laboratory experiment conducted in the Large Plasma Device (LAPD) at UCLA. Within this complex 3D evolution, it is more difficult to rigorously define and compute the reconnection rate. Strictly speaking, true topological changes in the magnetic field do not occur in these strong guide field systems, since all magnetic field lines map continuously from the cathode to the anode. However, both theory [3] and 3D simulations [3,4] have suggested that reconnection still occurs through the formation of quasiseparatrix layers (QSLs), which correspond to regions where neighboring field lines undergo rapid (but smooth) separations. When this separation rate is sufficiently rapid, one might naturally expect the plasma dynamics to resemble true (topological) separatrices. Recent simulations suggest that magnetic field lines passing through the quasiseparatrix layers are associated with large values of quasipotential computed by integrating $\Xi = \int_{\text{field line}} \vec{E} \cdot d\vec{l}$ along field lines. Indeed, within the generalized theory of magnetic reconnection [5], the maximum value of Ξ is a direct measure of the global nonlinear reconnection rate, and, thus, one would expect this to occur within the QSL [6]. Even within simulations, these ideas are challenging to verify, since they require mapping magnetic (and electric) fields through 3D volumes. However, with the unique capabilities available on LAPD, we have for the first time verified key aspects of quasiseparatrix reconnection in a laboratory experiment.

The experimental setup used to produce the magnetic ropes is shown in Fig. 1. The background plasma is on for 11 ms. Five ms after the background plasma is initiated, the flux ropes are switched on for 6 ms. The time at which the ropes are first generated is denoted by $t = 0$.

The background plasma density of $n = 1 \times 10^{12}$ cm^{-3} was measured with swept Langmuir probes calibrated using a 60 GHz microwave interferometer. The density in the center of the flux ropes is 4×10^{12} cm^{-3}. The flux-rope currents emanate from the LaB_6 cathode at the Alfvén speed and are collected on a mesh anode 11 m away. Several ms after the ropes are born, they become kink

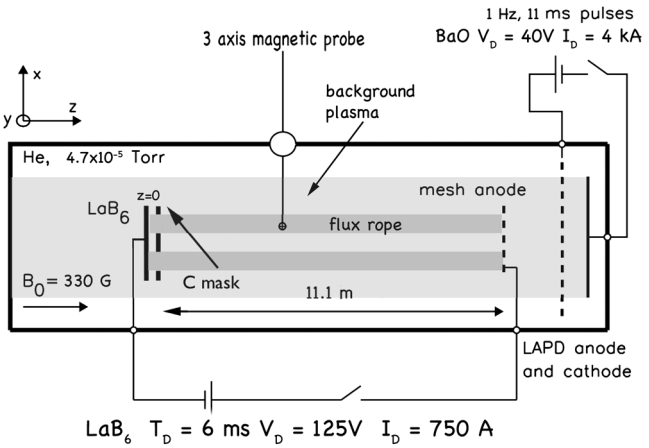

FIG. 1. Experimental setup (not to scale). The flux ropes are produced by emission of electron currents from a 20×20 cm LaB_6 cathode masked by a C plate with two 7.5 cm diameter holes, 3 cm edge to edge. The flux ropes are terminated on an anode 11 m away. The background plasma is produced independently with a BaO cathode producing a 17 m long plasma column 60 cm in diameter. The inner diameter of the vacuum vessel is 1 m. The coordinate system used places the source of the ropes at $z = 0$ and the center of the planes over which data were acquired as $x = y = 0$.

unstable and begin to bounce into one another. In the absence of strong axial flows, the threshold current for the kink instability (in mks) is given by [7]

$$I_{\text{kink}} = \frac{4\pi^2 R^2 B_0}{\mu_0 L}, \tag{1}$$

where R is the radius of a flux rope and L is its length. For a single rope, the threshold current is $I_{\text{kink}} = 133$ A, while the current in each rope is 375 A, and the radius of each rope varies between 3.75 and 6 cm depending on the axial location. In this experiment, the current must originate at the cathode (they are "line tied" to it) but can freely move about the mesh anode, which is a rectangle with sides of 25 and 28 cm and acts like a free boundary. The dispersion relation for a cylindrical flux rope, which can kink, is given by [7]

$$\tan(Lk_0\alpha) = -2i\alpha,$$
$$\text{where } \alpha = \sqrt{\frac{1}{4} + \left(\frac{\omega}{\sqrt{2}k_0 V_A}\right)^2}, \qquad k_0 = \frac{B_\theta}{RB_0}. \tag{2}$$

This was derived in the case for a flux rope anchored (line tied) at one end and free to move on the other end, which is the case in this experiment. For these conditions, $L = 11$ m and $V_A = 1.8 \times 10^5$ m/s. $[V_A = (B/\sqrt{\mu_0 n m_I})]$. Equation (2) was solved numerically using the measured range of R and $8G \le B_\theta \le 12G$, as these quantities vary between the source of the ropes and the anode. Using this range of R and B_θ, Eq. (2) predicts kink frequencies f_k between 4.7 and 7 kHz. The observed frequency of the oscillation of the ropes is 5.2 kHz.

Magnetic field data were acquired using 3 mm diameter magnetic (B-dot) probes wound on a form such that all three vector components of $\partial\vec{B}/\partial t$ were acquired. The probe moved to 2810 positions on each of 15 planes parallel to the background magnetic field ($\delta x = \delta y = 6$ mm) for a total of 42 100 spatial locations. The parallel planes were 64 cm apart. Ten shots were recorded at each x, y, z position (for a total of 421 000 experimental instances). A second magnetic probe fixed in space and in one of the ropes was used to calculate correlation functions for timing purposes [8]. A second emissive probe sensitive to the plasma potential [9] was moved to the same locations. Swept Langmuir probes were used on several planes to determine the plasma density and electron temperature. The electrostatic field was determined throughout the volume from $\vec{E}_{ES} = -\nabla V_p$. The induced electric field $\vec{E}_I = -(\partial\vec{A}/\partial t)$ was derived from the vector potential calculated from the three-dimensional currents $\vec{J} = (1/\mu_0)\nabla \times \vec{B}$. They are summed to calculate the total electric field throughout the volume and as a function of time. The time evolution of the 3D currents may be viewed in a movie in the Supplemental Material [10].

The squashing factor Q is a measure of spatial divergence of magnetic field lines, and its utility was first recognized by solar physicists studying the complex structures in the solar corona [11]. Isosurfaces of large Q are commonly referred to as QSLs. Within solar applications, the formation of a QSL is often associated with regions where magnetic energy is accumulating, eventually leading to onset. After reconnection is triggered, simulations have demonstrated the formation of intense QSLs associated with the nonlinear reconnection dynamics [3,12,13]. As illustrated in Fig. 2, by an isosurface corresponding to $Q = 100$, the observed QSL is similar in structure to a previous flux-rope experiment [14]. Following magnetic field lines for a small circle of seed points on the flux-rope source, the circle will map to an ellipse on their termination plane, with aspect ratio equal to the squashing factor $Q = 100$. Alternatively, the maximum separation distance between neighboring field lines on the initial circle will increase by a factor of $\sqrt{Q} = 10$.

The three-dimensional nature of the process is obvious in the anaglyph in Fig. 2 for fly around in 3D see Supplemental Material [10]. The currents circle around one or both of the ropes and close to the formation point about the QSL as well.

The experiment was designed such that the rope currents did not greatly exceed the kink condition, and the ropes subsequently do not behave chaotically as seen in a previous experiment [15]. In this case, the ropes periodically bounce into one another as illustrated in Fig. 3. The vertical plane in Fig. 3(a) illustrates the time development

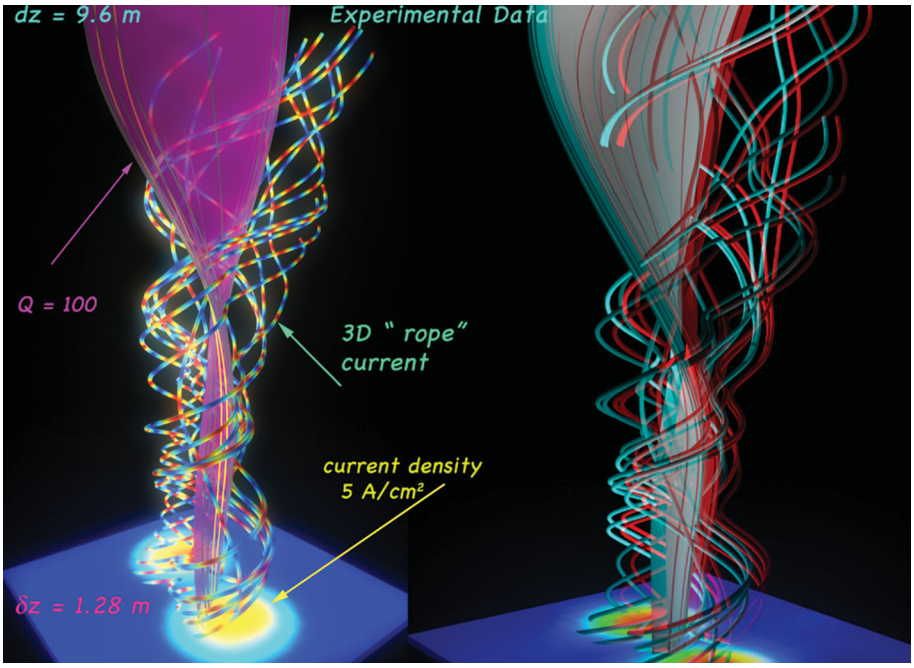

FIG. 2. The QSL shown as a magenta surface and current lines associated with the flux ropes. Several magnetic field lines are visible within the QSL. The bottom plane shows the current density of the two ropes 1.28 m from their origin. The picture on the right is an anaglyph or 3D image of the same, which can be viewed with readily available red and cyan glasses. A movie showing the 3D structure of the QSL from many camera angles is provided in Supplemental Material [10].

of $Q(x, t, y = 0)$ approximately in the center of the ropes at $z = 2.56$ m. Q can be as large as 500. The pattern of Fig. 3(a) oscillates at f_k; however, the field lines reconnect on a faster time scale. The reconnection time scale τ_{recon}, $\simeq 100$ μs was estimated by plotting $Q(t)$ at a location in which reconnection occurs. Figures 3(b) and 3(c) show the QSL on an x-y plane at $z = 2.56$ m. At the earlier time, the flux ropes are moving away from each other and Q is small. When the flux ropes collide as in Fig. 3(b), the squashing factor becomes large, of order $Q = 200$. The reconnection rate, or induced voltage, can be derived from the data by integrating the total electric field along the 3D magnetic field lines [16] as previously mentioned. This is done for the first time here because both components of the electric field and the magnetic field were measured throughout the volume making it possible to evaluate the integral along field lines. Ξ is shown in Fig. 3(d) at a time when the ropes collide. The "S-" shaped region in the center mirrors the QSL and has a value of $\Xi \simeq 6$ V. The region around the S has a voltage of opposite sign, which is most likely associated with circulating current. Figure 3(e) shows the measured power at a location inside the QSL when Q is large.

In the study of 3D reconnection, it is interesting to understand how the frozen-in condition is violated for field lines passing through the QSL. The parallel electron momentum equation in the fluid approximation may be written as

$$\frac{m_e}{e}\frac{dv_\parallel}{dt} = -E_\parallel - \frac{1}{ne}(\nabla \cdot P)_\parallel + \eta_\parallel \vec{J}_\parallel. \tag{3}$$

The term on the left has two components. The first of these terms $(m_e/e)(\partial v_\parallel/\partial t)$ is negligible because of the small electron mass, the low frequency of the rope oscillations, and because the electron drift in the rope currents are 1% of the electron thermal velocity. The convective derivative $((m_e/e)v_\parallel \cdot \nabla v_\parallel)$ is far less than the first term because the gradients in the current are small. The parallel pressure gradient was measured using the measured temperature and pressure on two planes separated in z by 3.2 m and $\int (1/ne)(\nabla \cdot P)_\parallel \cdot d\vec{l}$ evaluated by following field lines from one plane to the other is of order 0.5–1.2 V depending on the position in the plane. The integrated electric field along field lines $\int \vec{E} \cdot d\vec{l}$ is of order -0.5 to -1.0 V. Since both measurements are accurate to within 20%, we conclude that the electric field nearly balances the pressure gradient along field lines, with some remaining contribution balanced by the resistive term. An accurate measurement of the resistivity will require acquiring temperature and density on the same dense 3D grid that magnetic and electric fields were measured on. This will be the subject of a future study. It is interesting to note that recent 3D kinetic simulations have also concluded that the electron pressure tensor plays a key role in balancing the quasipotential [17].

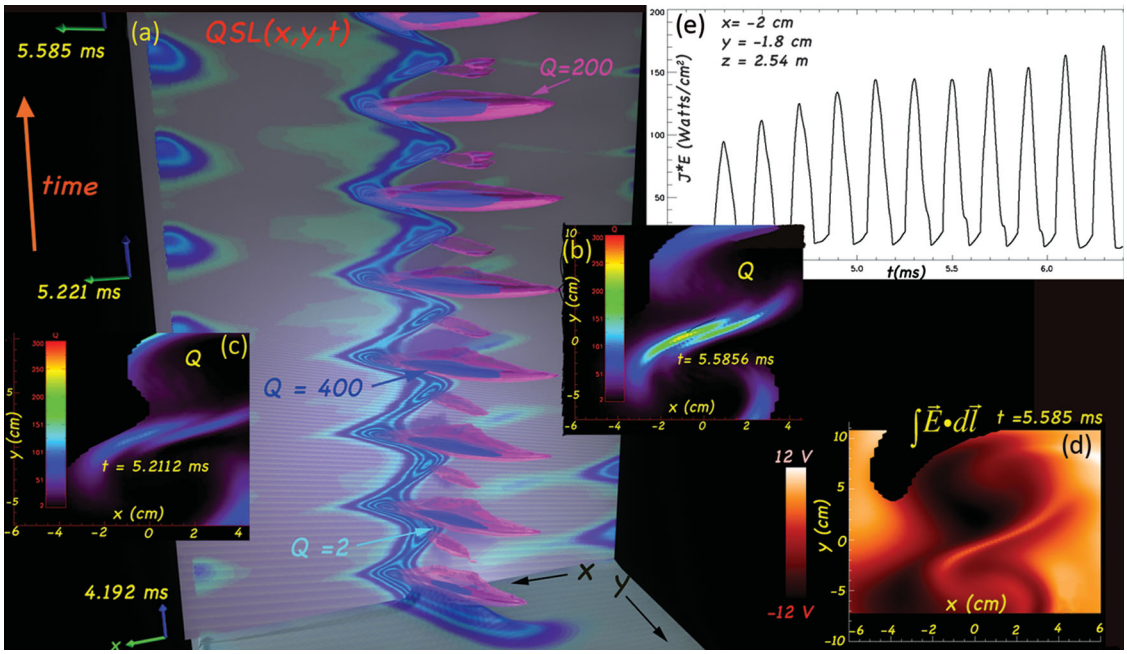

FIG. 3. (a) QSL on two cut planes. The vertical plane shows the time dependence of Q at $(-30 \le x \le 30$ cm, $y = 0$, $z = 2.56)$ and the vertical axis is time. The x-y plane shows the spatial dependence of Q at $t = 4.192$ ms. Two isosurfaces at $Q = 400$ and 200 are superimposed. (b) $Q(x, y, t_1 = 5.5856$ ms$)$ at $z = 2.56$ m, this is a time when the ropes collide. (c) $Q(x, y, t_2 = 5.521\,12$ ms$)$ at $z = 2.56$ m when Q is small. (d) The integral of the electric field along the magnetic field over the full $\delta z = 11$ m. This is a projection on an x-y plane at $\delta z = 2.56$ m. (e) The power density in W/cm^3 as a function of time at a location within the QSL. The estimated error in $\vec{J} \cdot \vec{E}$ is less than 20%.

The volume-averaged power $(1/V) \int \vec{J} \cdot \vec{E} dV$ spikes during a collision to 0.35 W/cm^3 but can locally be as high as 200 W/cm^3. While both the average and local power dissipation oscillate at the kink frequency, there is a time lag of $\sim$150 μs between the peak dissipated power within the QSL and the volume-averaged dissipated power, which is dominated by contributions from the much larger volume outside the QSL. The location of maximum Q in Fig. 3(b) is also associated with peak power dissipation [Fig. 3(e)]. The time evolution of this energy conversion and the QSL formation both track the heartbeat associated with the flux-rope collisions. When the flux ropes move apart, Q between the ropes drops. The data were searched for field lines, initially an electron skin depth apart, and moving towards one another at the ion sound speed (nearly the same as V_A based on the reconnection field) which had antiparallel components of magnetic field (B_x or B_y) of 0.11 G (100 times smaller than the field of the ropes themselves).

A rough estimate of the average energy (during the 50 μs reconnection burst) released by the annihilation of all the 0.11 G magnetic field for these was 4.62 J. If one compares this to the volume-averaged power during the seventh burst in Fig. 3(e), one gets a similar value, approximately 2 J, which depends upon the reconnection volume used. The steady state part of the power in Fig. 3(e) is most likely due to resistive power loss in the current sheet [the dc Joule heating is 20 kW (0.3 W/cm^3 vol of ropes), the rope discharge power is 93 kW].

Is the bulk of the reconnection occurring in the QSL? In this experiment, we hypothesize that the QSL between the currents is due to reconnection, and other QSLs at the periphery of the current channels are due to field lines associated with spreading currents. There are no nulls in the 3D magnetic field; the current is fully three dimensional (Fig. 2), and the classic "X" and "O" points associated with 2D reconnection are not present.

In order to better understand the spatial correlations between the QSL and the quasipotential, two isosurfaces of Ξ are shown in Fig. 4 with the values labeled. The positive value of Ξ is associated with the QSL and at this time overlaps about one-third of it. We associate negative values of Ξ with the electric field driving the flux-rope current. A second surface of $\Xi = -5$, which maps back to the source of the bottom flux rope, also exists below the QSL but was not drawn here as it would obscure the positive Ξ (blue surface) shown in Fig. 4. The full range of Ξ on a plane ($\delta z = 11$ m) is shown in Fig. 3(d). These results demonstrate that the field lines passing through the QSL are participating most strongly in the reconnection process. In the published literature, the nonlinear reconnection rate is often defined by the maximum value

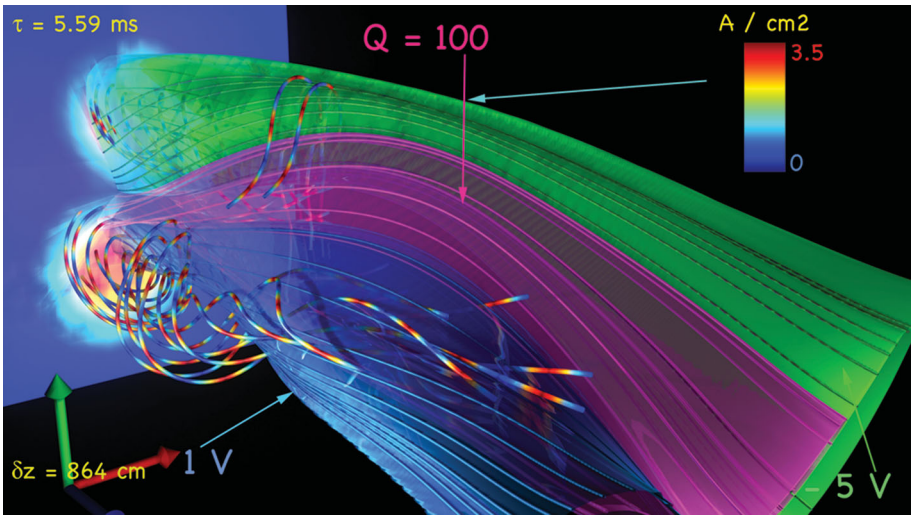

FIG. 4. QSL = 100 is shown in magenta during a flux-rope collision at $t = 5.5856$ ms. Diverging magnetic field lines within the QSL are visible. Also shown are two isosurfaces of the quasipotential Ξ, where the integration is performed along magnetic field lines starting at the flux-rope origin. Also shown is the flux-rope current density on a plane at $\delta z = 64$ cm. Several field lines of current (only shown in part of the volume) are drawn to aid the eye (also see Figs. 2 and 3).

of the quasipotential [5,6,12]. In order to compare with two-dimensional values of the reconnection rate, it is useful to define

$$R_r = \frac{\Xi}{LB_\theta V_A}, \tag{4}$$

which represents the average $\vec{E} \times \vec{B}$ inflow of flux into the QSL normalized by the Alfvén speed V_A computed with the reconnecting component of the field B_θ in the rope. For parameters in the experiments, $L = 11$ m is the length of the field line, $B_\theta \sim 10$ G, $n \approx 4 \times 10^{12}$ cm^{-3}, the Alfvénic reconnection rate is $R_r \sim 0.1$ which is close to the reconnection rates inferred from 3D kinetic simulations using the quasipotential [6,17].

Conclusions.—This is the first experiment on fully 3D reconnection to establish a causal link between the squashing factor and the quasipotential associated with reconnecting magnetic field lines. These results demonstrate a clear correlation between large values of the squashing factor and spikes in the reconnection rate inferred through the quasipotential. These correlations are observed during periods when the flux ropes are moving towards one another and are substantially less when the flux ropes are moving apart. These initial measurements suggest that the electron pressure gradient may provide a significant contribution to support the quasipotential, and in future experiments we will more carefully explore the relative contribution with the resistive term. The results in this Letter provide the first direct experimental test of reconnection within a QSL, where field-line mappings change continuously across a narrow region. Since this type of generalized reconnection does not require strict topological changes, it may be one of the most ubiquitous forms of reconnection in nature and is likely to occur even within turbulent cascades [18].

This research was done at the Basic Plasma Science Facility, which is supported by DOE under Grant No. DOE-DE-FC02-07ER54918:011 and NSF under Grant No. NSF-PHY-1036140. This research was sponsored by the U.S. Department of Energy, Office of Fusion Energy Sciences and the University of California Office of the President under Grant No. 12-LR-237124 from the UCOP program. The authors would like to acknowledge the valuable technical assistance of Z. Lucky and M. Drandell, as well as the contributions of J. Bonde and M. Martin.

[1] C. T. Russell, E. R. Priest, and L.-C. Lee, *1990 Physics of Magnetic Flux Ropes* AGU Geophysical Monograph Series Vol. 58 (American Geophysical Union, Washington, DC, 1990); S. Lukin, Self-organization in magnetic flux ropes, Plasma Phys. Controlled Fusion **56**, 060301 (2014).
[2] H. Furth, J. Killeen, and M. Rosenbluth, Finite-resistivity instabilities of a sheet pinch, Phys. Fluids **6**, 459 (1963).
[3] P. Démoulin, Extending the concept of seperatricies to QSLs for magnetic reconnection, Adv. Space Res. **37**, 1269 (2006).
[4] E. R. Priest and P. Démoulin, Three-dimensional magnetic reconnection without null points, J. Geophys. Res. **100**, 23443 (1995); V. S. Titov, G. Hornig, and P. Démoulin, Theory of magnetic connectivity in the solar corona, J. Geophys. Res. **107**, SSH 3-1 (2002).
[5] M. Hesse, T. Forbes, and J. Birn, On the relation between reconnected magnetic flux and parallel electric fields in the solar corona, Astrophys. J. **631**, 1227 (2005).
[6] D. E. Wendel, D. K. Olson, M. Hesse, N. Aunai, M. Kuznetsova, H. Karimabadi, W. Daughton, and M. L. Adrian, The relation between reconnected flux, the parallel

electric field, and the reconnection rate in a three-dimensional kinetic simulation of magnetic reconnection, Phys. Plasmas **20**, 122105 (2013).

[7] D. Ruytov, I. Furno, T. Intrator, S. Abbate, and T. Madziwa-Nussinov, Phenomenological theory of the kink instability in a slender plasma column, Phys. Plasmas **13**, 032105 (2006).

[8] T. DeHaas, W. Gekelman, and B. Van Compernolle, Experimental study of a linear/non-linear flux rope, Phys. Plasmas **22**, 082118 (2015).

[9] M. J. Martin, J. Bonde, W. Gekelman, and P. Pribyl, A resistively heated CeB_6 emissive probe, Rev. Sci. Instrum. **86**, 053507 (2015).

[10] See Supplemental Material at http://link.aps.org/supplemental/10.1103/PhysRevLett.116.235101 for more details.

[11] V. S. Titov, K. Galsgaard, and T. Neukirch, Magnetic pinching of hyperbolic flux tubes. I. basic estimations, Astrophys. J. **582**, 1172 (2003); C. H. Mandrini, P. Démoulin, L. Driel-Gesztelyi, B. Schmieder, G. Cauzzi, and A. Hofmann, 3D magnetic reconnection at an X-ray bright point, Sol. Phys. **168**, 115 (1996); V. S. Titov and G. Horning, Theory of magnetic connectivity in the solar corona, J. Geophys. Res. **107**, SSH 3-1 (2002).

[12] J. M. Finn, Z. Billey, W. Daughton, and E. Zweibel, Quasi-separatrix layer reconnection for nonlinear line-tied collisionless tearing modes, Plasma Phys. Controlled Fusion **56**, 064013 (2014).

[13] W. Daughton, T. K. M. Nakamura, H. Karimabadi, V. Roytershteyn, and B. Loring, Computing the reconnection rate in turbulent kinetic layers by using electron mixing to identify topology, Phys. Plasmas **21**, 052307 (2014).

[14] E. E. Lawrence and W. Gekelman, Identification of a Quasiseparatrix Layer in a Reconnecting Laboratory Magnetoplasma, Phys. Rev. Lett. **103**, 105002 (2009).

[15] W. Gekelman, B. Van Compernolle, T. DeHaas, and S. Vincena, Chaos in magnetic flux ropes, Plasma Phys. Controlled Fusion **56**, 064002 (2014).

[16] M. Hesse, T. Forbes, and J. Birn, On the relation between reconnected magnetic flux and parallel electric fields in the solar corona, Astrophys. J. **631**, 1227 (2005).

[17] Y.-H. Liu, W. Daughton, H. Li, H. Karimabadi, and V. Roytershteyn, Bifurcated Structure of the Electron Diffusion Region in Three-Dimensional Magnetic Reconnection, Phys. Rev. Lett. **110**, 265004 (2013).

[18] M. Wan, W. H. Matthaeus, V. Roytershteyn, H. Karimabdai, T. Parashar, P. Wu, and M. Shay, Intermittent Dissipation and Heating in 3D Kinetic Plasma Turbulence, Phys. Rev. Lett. **114**, 175002 (2015).